Mathematical Modelling of Cervical Cancer with HPV infection
PROJECT – REPORT

By
Abhishek Pal/856
Aditya Vishwakarma/860
Amit Chausali/866
Arindam Mondal/880

Under the guidance of
Dr. Sudeshna Mondal

Abstract

Cervical cancer is one of the most prevalent cancers among women worldwide, with over 600,000 new cases and more than 340,000 deaths reported annually. More than 95% of cervical cancer cases are attributed to persistent infections with high-risk human papillomavirus(HPV). The disease burden is significantly higher in low- and middle-income countries, where access to screening and vaccination remains limited.In this paper, we develop and analyze a compartmental mathematical model to understand the transmission dynamics of HPV and its progression to cervical cancer. The population is categorized into four compartments: susceptible (S), infected (I), cancer (C), and recovered (R) individuals. The model incorporates key epidemiological parameters, including the transmission rate, progression rate to cancer, recovery rate, and natural mortality. By applying the next-generation matrix method, we determine the basic reproduction number (R_0), which serves as a threshold parameter indicating whether the disease persists or is eradicated. Numerical simulations using realistic population data demonstrate that when $R_0 < 1$, the disease-free equilibrium is globally asymptotically stable, leading to infection elimination. Conversely, when $R_0 > 1$, the model stabilizes at an endemic equilibrium, where infection and cancer persist at steady levels.

1 Introduction

Cervical cancer, primarily caused by persistent infection with high-risk human papillomavirus (HPV) strains, remains a major global health challenge. According to the World Health Organization (WHO), cervical cancer is the fourth most common cancer among women, with an estimated 600,000 new cases and 340,000 deaths reported globally in 2023 [1]. Despite advances in early detection and preventive measures, disparities in healthcare accessibility continue to contribute to high morbidity and mortality rates [2]. The disease is particularly prevalent in low- and middle-income countries where HPV vaccination and screening programs remain insufficient [3].

Mathematical modeling has emerged as a crucial tool in understanding disease progression, optimizing resource allocation, and guiding public health policies. Compartmental epidemiological models classify populations based on disease status and provide valuable insights into the transmission dynamics of infectious diseases [4]. Traditional models, such as the susceptible-infected-recovered (SIR) framework, have been extensively used for diseases like tuberculosis and COVID-19 [5]. However, cervical cancer progression involves multiple biological and behavioral factors, requiring more complex modeling approaches.

Several studies have expanded upon the standard SIR framework by incorporating additional compartments representing HPV infection stages, cervical intraepithelial neoplasia (CIN), and cancer progression [6]. These models have been applied to different population settings, particularly high-risk regions such as Sub-Saharan Africa and Southeast Asia, where HPV prevalence is significantly high [7]. Furthermore, research indicates that early screening and vaccination programs significantly impact disease outcomes [8].

Despite the insights gained from compartmental models, their predictive capabilities are often limited by assumptions about disease progression and population dynamics. To address these challenges, data-driven approaches, including machine learning and deep learning models, have been increasingly utilized in cervical cancer research [9]. These models leverage large-scale epidemiological datasets to identify hidden patterns and predict disease trends more accurately. Studies have shown the effectiveness of deep learning in predicting HPV infection persistence and optimizing screening strategies in resource-limited settings [10]. However, while data-driven methods offer flexibility, they are prone to overfitting and often lack mechanistic disease progression insights.

To bridge the gap between mechanistic and data-driven approaches, recent research has integrated epidemiological models with deep learning techniques. Hybrid frameworks that combine compartmental disease models with neural networks enhance predictive accuracy while maintaining epidemiological interpretability [11]. In the context of cervical cancer, such models incorporate factors like vaccination coverage, screening rates, and demographic influences to improve early detection and intervention strategies. Additionally, network-based models have been employed to capture spatial heterogeneity and population interactions, enabling more precise predictions of HPV transmission dynamics [12].

Given the global burden of cervical cancer and the need for efficient intervention strategies, mathematical modeling remains an essential tool in guiding public health policies. Future research should focus on improving predictive accuracy by incorporating real-world data and refining hybrid models to enhance decision-making in HPV prevention and control.

2 Mathematical model formulation of cervical cancer

The dynamics of the population is governed by the following system of equations:

$$\begin{aligned}
\frac{dS}{dt} &= \Lambda - \frac{\beta SI}{1 + \alpha' I} - \mu S + \alpha R \\
\frac{dI}{dt} &= \frac{\beta SI}{1 + \alpha' I} - \gamma I - \delta I - \mu I \\
\frac{dC}{dt} &= \delta I - \xi C - \mu C \\
\frac{dR}{dt} &= \gamma I - \alpha R - \mu R
\end{aligned} \tag{2.1}$$

with initial conditions

$$S(0) > 0, \ I(0) \geq 0, \ C(0) \geq 0, \ R(0) \geq 0 \tag{2.2}$$

where

Variable	Description
$S(t)$	Susceptible population
$I(t)$	Infected population (with HPV infection)
$C(t)$	Cancer population (with cervical cancer)
$R(t)$	Recovered population (after HPV infection)

Table 1: Description of variables

Parameter	Description
Λ	Rate of new individuals entering the susceptible population
β	Transmission rate of HPV infection
α	Rate of immunity loss in recovered individuals
α'	Saturation factor
γ	Recovery rate from HPV infection
δ	Rate of progression from infection to cancer
ξ	Recovery rate from cervical cancer
μ	Natural mortality rate

Table 2: Description of biologically meaningful parameters

3 Positivity and Uniform boundedness

Theorem 3.1. *The solutions $(S(t), I(t), C(t), R(t))$ of the system (2.1) remain nonnegative for all $t > 0$ with the initial conditions $S(0) > 0$ and $I(0), C(0), R(0) \geq 0$.*

Proof. From first equation of system (2.1), we start with the given differential equation neglecting αR:

$$\frac{dS}{dt} \geq \Lambda - \frac{\beta I S}{1 + \alpha' I} - \mu S$$

$$\Rightarrow \frac{dS}{dt} \geq \Lambda - \beta S I - \mu S \left[\text{ since } -\frac{\beta S I}{1 + \alpha' I} \geq -\beta S I \right]$$

$$\therefore \frac{dS}{dt} + (\beta I + \mu)S \geq \Lambda$$

$$\Rightarrow S(t) \geq S(0) \exp\left(-\int_0^t \beta I(v)dv - \mu t \right) + \exp\left(-\int_0^t \beta I(v)dv - \mu t \right) \times$$

$$\int_0^t \Lambda \exp\left(\int_0^z \beta I(v)dv + \mu z \right) dz > 0 \, [\text{ since } S(0) > 0]$$

Now, from second equation of system (2.1), we start with the given differential equation neglecting $\frac{\beta S I}{1 + \alpha' I}$:

$$\frac{dI}{dt} + (\mu + \gamma + \delta)I \geq 0$$

$$\Rightarrow \frac{dI}{I} + (\mu + \gamma + \delta)dt \geq 0.$$

Integrating both sides, we have:

$$\int_{I(0)}^{I(t)} \frac{dI}{I} \geq -\int_{u=0}^t (\mu + \gamma + \delta)du$$

$$\Rightarrow I(t) \geq I(0) \, \exp(-(\mu + \gamma + \delta)t)$$

$\therefore$ $I(t) \geq 0$, since $I(0) \geq 0$.

From third equation of system (2.1), we start with the given differential equation neglecting δI:

$$\frac{dC}{dt} \geq -(\zeta + \mu)C.$$

$$\Rightarrow C(t) \geq C(0)\exp(-(\zeta + \mu)t)$$

$\therefore$ $C(t) \geq 0$, since $C(0) \geq 0$.

From fourth equation of system (2.1), we start with the given differential equation neglecting γI:

$$\frac{dR}{dt} + (\alpha + \mu)R \geq 0.$$

4

$$\Rightarrow R(t) \geq R(0) \exp(-(\alpha + \mu)t).$$

$\therefore$ $R(t) \geq 0$, since $R(0) \geq 0$.

Hence, the proof. $\qquad\qquad\qquad\qquad\qquad\qquad\qquad\qquad\qquad\qquad\qquad$ $\square$

Theorem 3.2. *Let $(S(t), I(t), C(t), R(t))$ be any solution of the model (2.1) with (2.2) in $\mathbb{R}_+^4$, then the feasible region*

$$\Omega = \left\{ (S(t), I(t), C(t), R(t)) \in \mathbb{R}_+^4 : 0 < N(t) < \frac{\Lambda}{\mu} + \epsilon, \ \epsilon > 0 \right\}$$

Proof. The total population is defined as:

$$N(t) = S(t) + I(t) + C(t) + R(t).$$

Differentiating both sides w.r.t. t, we have:

$$
\begin{aligned}
\frac{dN}{dt} &= \frac{dS}{dt} + \frac{dI}{dt} + \frac{dC}{dt} + \frac{dR}{dt} \\
&= \Lambda - \mu S - \mu I - \mu R - \mu C - \zeta C \\
&= \Lambda - \mu N - \zeta C \\
&\leq \Lambda - \mu N.
\end{aligned}
$$

$$
\begin{aligned}
\therefore \frac{dN}{dt} + \mu N &\leq \Lambda \\
\Rightarrow N(t)e^{\mu t} &\leq \frac{\Lambda}{\mu}e^{\mu t} + \text{ constant} \\
\Rightarrow N(t) &\leq N(0)e^{-\mu t} + \frac{\Lambda}{\mu}\left(1 - e^{-\mu t}\right).
\end{aligned}
$$

$\therefore$ $0 < N(t) < \frac{\Lambda}{\mu} + \epsilon$ for $t \to \infty$ and $\epsilon > 0$.

A globally attractive system means that regardless of the initial population sizes, the system always converges to a steady state over time. Thus, in the long run, the distribution of susceptible, infected, cancer, and recovered individuals stabilizes, and the population does not grow or shrink indefinitely.

$\qquad\qquad\qquad\qquad\qquad\qquad\qquad\qquad\qquad\qquad\qquad\qquad\qquad\qquad\qquad$ $\square$

4 Equilibrium Points

To analyze the equilibrium states of the model, we solve for the disease-free equilibrium (DFE) and endemic equilibrium (EE) points, based on the mathematical model described in the paper.

Disease-free equilibrium (DFE)

occurs when there are no infections in the population, i.e., $I = 0$ and $C = 0$. Setting the system of equations to zero:

$$S^* = \frac{\Lambda}{\mu}, \qquad I^* = 0, \quad C^* = 0, \quad R^* = 0.$$

This represents the state where no infection exists, and the susceptible population remains at a stable level determined by the birth and death rates.

Endemic equilibrium (EE)

occurs when the infection persists in the population, meaning $I^* \neq 0$ and $C^* \neq 0$. The endemic equilibrium points are given by:

$$S^* = \frac{(\delta + \gamma + \mu)(1 + \alpha' I)}{\beta}, \quad I^* = \frac{(\Lambda\beta - \mu(\delta + \gamma + \mu))(\alpha + \mu)}{\beta[(\alpha + \mu)(\delta + \gamma + \mu) - \alpha\delta] + \alpha'\mu(\alpha + \mu)(\gamma + \delta + \mu)},$$

$$C^* = \frac{\delta I^*}{\xi + \mu}, \quad R^* = \frac{\gamma I^*}{\alpha + \mu}.$$

These equations describe the steady-state levels of each compartment when the disease remains endemic in the population.

5   Basic reproduction number and its computation

The basic reproduction number (denoted by R_0) is the estimated number of secondary cases created by a typical infected person during its entire cycle of infectiousness in a fully susceptible population. We calculate the basic reproduction number of the model using the method of the next-generation matrix developed by Van den Driessche and Watmough.

New Infections (F)

New infections enter the system through the infected compartment (I) as follows:

1. Infection arises in the I compartment from susceptible individuals through transmission: $\frac{\beta S}{1 + \alpha' I}$.

2. No new infection occurs directly in the cancer compartment (C) directly .

3. The new infection function F includes only the infected compartment:

$$F = \begin{bmatrix} \frac{\beta S}{1 + \alpha' I} & 0 \\ 0 & 0 \end{bmatrix}.$$

Transition Matrix (V)

The transition matrix captures the rates of progression, recovery, and death out of infected compartments (I and C):

$$V = \begin{bmatrix} (\delta + \gamma + \mu) & 0 \\ -\delta & (\xi + \mu) \end{bmatrix}.$$

The inverse of the transition matrix is:

$$V^{-1} = \begin{bmatrix} \frac{1}{\delta + \gamma + \mu} & 0 \\ \frac{\delta}{(\delta + \gamma + \mu)(\xi + \mu)} & \frac{1}{\xi + \mu} \end{bmatrix}.$$

Next-Generation Matrix and Basic Reproduction Number

$$FV^{-1} = \begin{bmatrix} \frac{\beta S_0}{\delta + \gamma + \mu} & 0 \\ 0 & 0 \end{bmatrix}.$$

Thus, the basic reproduction number is:

$$R_0 = \frac{\beta S_0}{\delta + \gamma + \mu}.$$

Substituting the disease-free equilibrium value $S_0 = \frac{\Lambda}{\mu}$, we get:

$$R_0 = \frac{\beta \Lambda}{\mu(\delta + \gamma + \mu)}.$$

6 Stability analysis for a disease-free and Endemic equilibrium

6.1 Local stability

Theorem 6.1. *The disease-free equilibrium E_0 of the model is locally asymptotically stable if $R_0 < 1$ and unstable if $R_0 > 1$.*

Proof. The Jacobian matrix at E_0 is given by:

$$J(E_0) = \begin{bmatrix} -\mu & -\frac{\beta \Lambda}{\mu} & 0 & \alpha \\ 0 & \frac{\beta \Lambda}{\mu} - (\delta + \gamma + \mu) & 0 & 0 \\ 0 & \delta & -(\xi + \mu) & 0 \\ 0 & \gamma & 0 & -(\alpha + \mu) \end{bmatrix}.$$

The characteristic roots are:

$$\lambda_1 = -\mu (< 0),$$
$$\lambda_2 = \frac{\beta \Lambda}{\mu} - (\delta + \gamma + \mu),$$
$$\lambda_3 = -(\xi + \mu)(< 0),$$
$$\lambda_4 = -(\alpha + \mu)(< 0).$$

For stability, real parts of all eigenvalues should be negative. So for the stability of E_0, λ_2 must be negative i.e., $\lambda_2 = \frac{\beta \Lambda}{\mu} - (\delta + \gamma + \mu) < 0 \Rightarrow \frac{\beta \Lambda}{\mu} < (\delta + \gamma + \mu)$ which gives the condition:

$$R_0 = \frac{\beta \Lambda}{\mu(\delta + \gamma + \mu)} < 1$$

In summary, when $\lambda_2 < 0$, the disease cannot invade or persist in the population, and the system settles at the disease-free equilibrium. Understanding this threshold helps guide public health interventions to keep R_0 below 1, effectively eradicating the infection.

Conversely, when $\lambda_2 > 0$ and $R_0 > 1$, the disease-free equilibrium E_0 becomes unstable.

$\square$

Theorem 6.2. *The endemic equilibrium $E_1(S^*, I^*, C^*, R^*)$ is locally asymptotically stable if $R_0 > 1$, and unstable if $R_0 < 1$.*

Proof. The Jacobian matrix at $E_1(S^*, I^*, C^*, R^*)$ is given by:

$$J(E_1) = \begin{bmatrix} -\frac{\beta I^*}{1+\alpha' I^*} - \mu & -\frac{\beta S^*}{(1+\alpha' I^*)^2} & 0 & \alpha \\ \frac{\beta I^*}{1+\alpha' I^*} & \frac{\beta S^*}{(1+\alpha' I^*)^2} - (\gamma + \delta + \mu) & 0 & 0 \\ 0 & \delta & -(\zeta + \mu) & 0 \\ 0 & \gamma & 0 & -(\alpha + \mu) \end{bmatrix}.$$

The characteristic equation of $J(E_1)$ is:

$$\lambda^4 + a_1 \lambda^3 + a_2 \lambda^2 + a_3 \lambda + a_4 = 0,$$

$a_1 = -(a_{11} + a_{22} + a_{33} + a_{44}),$

$a_2 = (a_{33}a_{44} + a_{11}a_{44} + a_{11}a_{22} - a_{12}a_{21} + a_{11}a_{33} + a_{22}a_{44} + a_{22}a_{33}),$

$a_3 = -(a_{22}a_{33}a_{44} + a_{11}a_{33}a_{44} + a_{11}a_{22}a_{44} - a_{12}a_{21}a_{44} + a_{14}a_{21}a_{42} + a_{11}a_{22}a_{33} - a_{12}a_{21}a_{33}),$

$a_4 = a_{11}a_{22}a_{33}a_{44} - a_{12}a_{21}a_{33}a_{44} + a_{14}a_{21}a_{33}a_{42},$

$a_{11} = -\frac{\beta I^*}{1+\alpha' I^*} - \mu, a_{12} = -\frac{\beta S^*}{(1+\alpha' I^*)^2}, a_{14} = \alpha, a_{21} = \frac{\beta I^*}{1+\alpha' I^*}, a_{22} = \frac{\beta S^*}{(1+\alpha' I^*)^2} - (\gamma + \delta + \mu),$

$a_{32} = \delta, a_{33} = -(\zeta + \mu), a_{42} = \gamma, a_{44} = -(\alpha + \mu).$

We observe that if $R_0 > 1$, the following conditions (Routh-Hurwitz criterion) hold:

$$a_1 > 0, \qquad a_2 > 0,$$
$$a_3 > 0, \qquad a_4 > 0,$$
$$a_1 a_2 a_3 > a_3^2 + a_1^2 a_4.$$

Thus, all the roots of the characteristic equation have negative real parts, implying that the endemic equilibrium is locally asymptotically stable when $R_0 > 1$.

$\square$

6.2 Global stability

Theorem 6.3. *The disease-free equilibrium E_0 of model (2.1) is globally asymptotically stable if $R_0 < 1$.*

Proof. To establish the global stability of E_0, we construct a Lyapunov function:

$$V(t) = I(t) + aC(t),$$

where $a > 0$ is a constant to be determined. Differentiating $V(t)$ with respect to time, we obtain:

$$\frac{dV}{dt} = \frac{dI}{dt} + a\frac{dC}{dt}.$$

From the given system:

$$\frac{dI}{dt} = \frac{\beta SI}{1 + \alpha' I} - (\gamma + \delta + \mu)I,$$

8

$$\frac{dC}{dt} = \delta I - (\xi + \mu)C.$$

Substituting these into $\frac{dV}{dt}$:

$$\frac{dV}{dt} = \frac{\beta SI}{1 + \alpha' I} - (\gamma + \delta + \mu)I + a\left(\delta I - (\xi + \mu)C\right).$$

At $E_0 = (S_0, 0, 0, 0)$, where $S_0 = \frac{\Lambda}{\mu}$, we use $R_0 = \frac{\beta\Lambda}{\mu(\delta+\gamma+\mu)}$.
Rewriting $\frac{dV}{dt}$:

$$
\begin{aligned}
\frac{dV}{dt} &= \left(\frac{\beta S_0}{1 + \alpha' I} - (\delta + \gamma + \mu) + a\delta\right) I - a(\xi + \mu)C \\
&\leq \left[\beta S_0 - (\delta + \gamma + \mu) + a\delta\right] I \\
&= \left[\beta \frac{\Lambda}{\mu} - (\delta + \gamma + \mu) + a\delta\right] I \\
&= \left[(R_0 - 1)(\gamma + \delta + \mu) + a\delta\right] I.
\end{aligned}
$$

Now, choosing $a = R_0 - 1$, we obtain:

$$\frac{dV}{dt} = (R_0 - 1)(2\delta + \gamma + \mu)I.$$

Since $R_0 < 1$, it follows that $\frac{dV}{dt} < 0$, which ensures that the disease-free equilibrium E_0 is globally asymptotically stable by LaSalle's Invariance Principle.

Thus when $R_0 < 1$, the infection will eventually die out, and the population will return to the disease-free equilibrium. □

Theorem 6: The endemic equilibrium E_1 of our model is globally asymptotically stable, provided the following conditions hold:

$$I > I^*, \qquad\qquad R > R^*, \qquad SI^* < S^* I,$$
$$2 - \frac{C^*}{C} - \frac{R^*}{R} < 0, \qquad 1 + I - I^* - \frac{S^*}{S} < 0$$

Proof. We construct a Lyapunov function to establish the global stability of E_1:

$$
\begin{aligned}
V(t) &= \left(S - S^* - S^* \ln \frac{S}{S^*}\right) + \left(I - I^* - I^* \ln \frac{I}{I^*}\right) + \frac{\alpha + \mu}{\delta}\left(C - C^* - C^* \ln \frac{C}{C^*}\right) \\
&\quad + \frac{\alpha + \mu}{\gamma}\left(R - R^* - R^* \ln \frac{R}{R^*}\right) + \frac{\alpha}{2\gamma}(R - R^*)^2.
\end{aligned}
$$

Differentiating $V(t)$, we have:

$$\frac{dV}{dt} = \left(1 - \frac{S^*}{S}\right)\frac{dS}{dt} + \left(1 - \frac{I^*}{I}\right)\frac{dI}{dt} + \frac{\alpha + \mu}{\delta}\left(1 - \frac{C^*}{C}\right)\frac{dC}{dt} + \frac{\alpha + \mu}{\gamma}\left(1 - \frac{R^*}{R}\right)\frac{dR}{dt} + \frac{\alpha}{\gamma}(R - R^*)\frac{dR}{dt}$$

$$\Rightarrow \frac{dV}{dt} = \left(1 - \frac{S^*}{S}\right)\left(\frac{\beta S^* I^*}{1 + \alpha' I^*} - \frac{\beta SI}{1 + \alpha' I} - \mu(S - S^*) + \alpha(R - R^*)\right) + (I - I^*)\left(\frac{\beta S}{1 + \alpha' I} - \frac{\beta S^*}{1 + \alpha' I^*}\right)$$

9

$$+(\alpha+\mu)\left(1-\frac{C^*}{C}\right)(I-I^*)-\frac{(\alpha+\mu)(\zeta+\mu)(C-C^*)^2}{\delta C}+(\alpha+\mu)\left(1-\frac{R^*}{R}\right)(I-I^*)-\frac{(\alpha+\mu)^2(R-R^*)^2}{R\gamma}$$

$$+\alpha(R-R^*)(I-I^*)-\frac{\alpha(\alpha+\mu)(R-R^*)^2}{\gamma},$$

since $\Lambda=\frac{\beta S^*I^*}{1+\alpha'I^*}+\mu S^*-\alpha R^*,\ \frac{\beta S^*}{1+\alpha'I^*}=\gamma+\delta+\mu,\ \delta I^*-(\zeta+\mu)C^*=0,\ \gamma I^*-(\alpha+\mu)R^*=0$

$$\Rightarrow\frac{dV}{dt}\leq\left(1-\frac{S^*}{S}\right)\left(\frac{\beta S^*I^*}{1+\alpha'I^*}-\frac{\beta SI}{1+\alpha'I}-\mu(S-S^*)+\alpha(R-R^*)\right)+(I-I^*)\left(\frac{\beta S}{1+\alpha'I}-\frac{\beta S^*}{1+\alpha'I^*}\right)$$

$$+(\alpha+\mu)\left(1-\frac{C^*}{C}\right)(I-I^*)+(\alpha+\mu)\left(1-\frac{R^*}{R}\right)(I-I^*)+\alpha(R-R^*)(I-I^*),$$

$$\Rightarrow\leq-\beta(SI-S^*I^*)\left(1-\frac{S^*}{S}\right)-\alpha'\beta II^*\frac{(S-S^*)^2}{S}+\beta(S-S^*)(I-I^*)+\alpha'\beta(I-I^*)(SI^*-S^*I)-\mu\frac{(S-S^*)^2}{S}$$

$$+(\alpha+\mu)(I-I^*)\left(2-\frac{C^*}{C}-\frac{R^*}{R}\right)+\alpha(R-R^*)\left(1+I-I^*-\frac{S^*}{S}\right),\ \text{since}\ \frac{1}{1+\alpha'I}\leq1,\ \frac{1}{1+\alpha'I^*}\leq1$$

$$\Rightarrow=-\beta I^*\frac{(S-S^*)^2}{S}-\alpha'\beta II^*\frac{(S-S^*)^2}{S}+\alpha'\beta(I-I^*)(SI^*-S^*I)-\mu\frac{(S-S^*)^2}{S}$$

$$+(\alpha+\mu)(I-I^*)\left(2-\frac{C^*}{C}-\frac{R^*}{R}\right)+\alpha(R-R^*)\left(1+I-I^*-\frac{S^*}{S}\right).$$

$\therefore\frac{dV}{dt}<0$ if we take $I>I^*,R>R^*,SI^*<S^*I,2-\frac{C^*}{C}-\frac{R^*}{R}<0$ and $1+I-I^*-\frac{S^*}{S}<0$ and $\frac{dV}{dt}=0$ at $S=S^*,I=I^*,C=C^*,R=R^*$.

Hence, by LaSalle's Invariance Principle, $E_1(S^*,I^*,C^*,R^*)$ is globally asymptotically stable under the conditions $\left\{I>I^*,R>R^*,SI^*<S^*I,2-\frac{C^*}{C}-\frac{R^*}{R}<0,1+I-I^*-\frac{S^*}{S}<0\right\}$.

$\square$

7 Transcritical Bifurcation Analysis

A transcritical bifurcation is a type of local bifurcation where two fixed points collide and exchange their stability. This occurs when a parameter crosses a critical value, causing a qualitative change in the behavior of the system's fixed points.

In our study, this occurs when the disease-free equilibrium E_0 and the endemic equilibrium E_1 exchange stability when they cross the line $R_0=1$.

- For $R_0<1$, only E_0 is stable.

- For $R_0 > 1$, E_1 becomes stable.

To analyze the bifurcation, we examine the stability and existence of equilibrium at $R_0 = 1$ using the Jacobian matrix and center manifold theory.
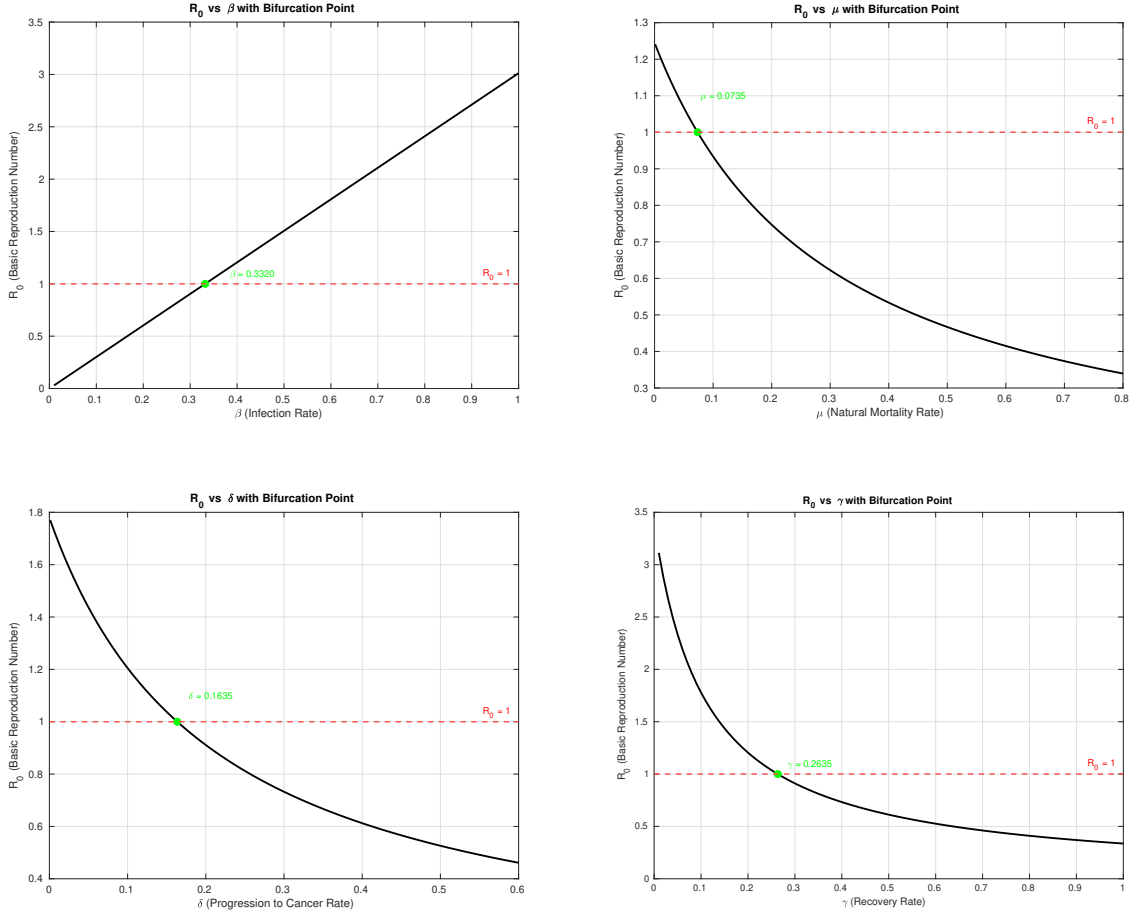

Figure 1: Transcritical bifurcation diagrams with respect to system parameters

Stability regions of parameters for the disease-free and Endemic Equilibrium
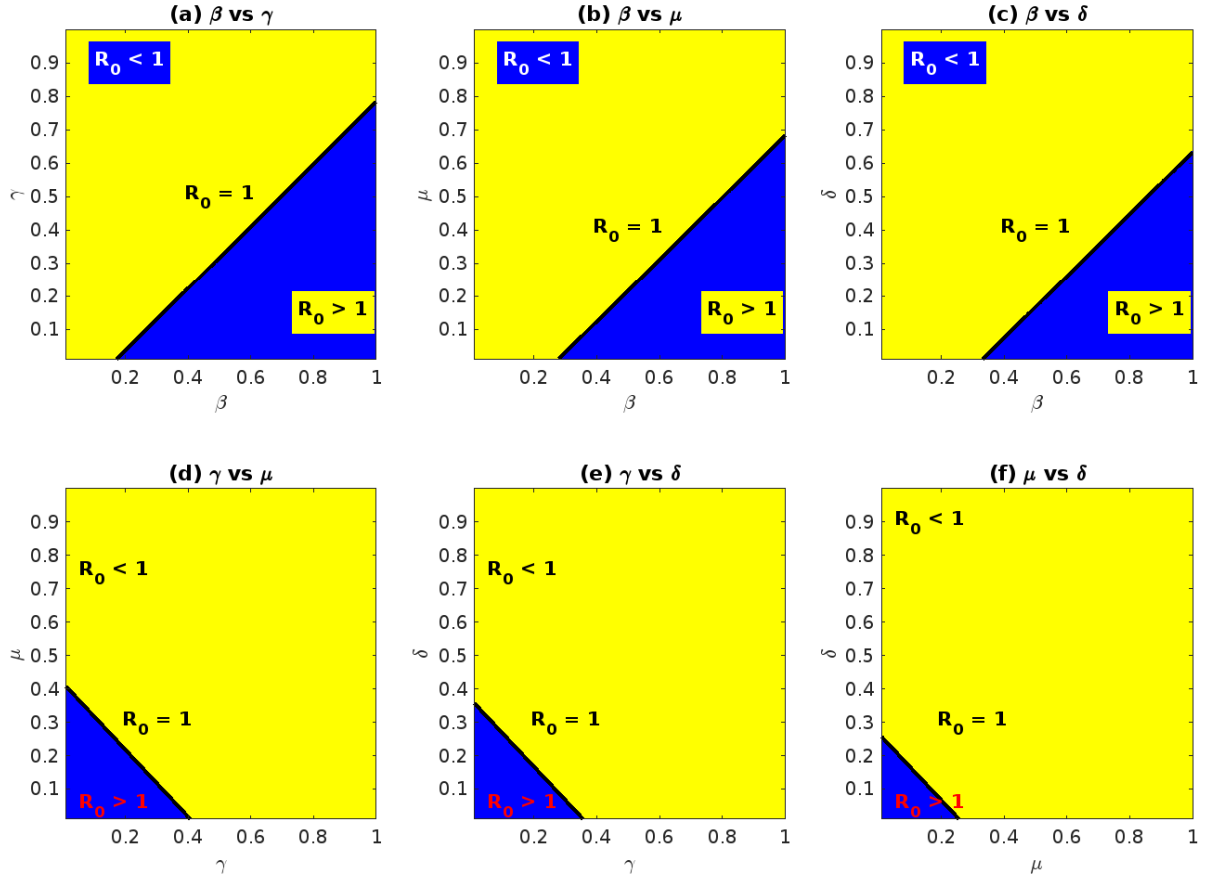
Figure 2: Two parameters bifurcation diagrams

8 Sensitivity analysis

Sensitivity analysis helps us understand how changes in model parameters affect the output of a mathematical model. In epidemiological models (like yours for HPV and cervical cancer), this tells us which parameters have the most influence on things like the basic reproduction number or endemic equilibrium.

Local sensitivity index

We compute the sensitivity indices of the basic reproduction number R_0 to identify the parameters with the most significant impact. This helps determine which factors should be targeted to improve intervention strategies. The normalized forward sensitivity index of a variable L that depends on the differentiability of a parameter p is defined as:

$$\Upsilon_{R_0}^p = \frac{p}{R_0} \times \frac{\partial R_0}{\partial p}.$$

Including the immunity loss parameter α, the sensitivity indices of R_0 with respect to the model parameters become:

$$\Upsilon_{R_0}^{\beta} = 1, \qquad \qquad \text{(Transmission rate)}$$

$$\Upsilon_{R_0}^{\Lambda} = 1, \qquad \qquad \text{(Recruitment rate)}$$

$$\Upsilon_{R_0}^{\gamma} = -\frac{\gamma}{\delta + \gamma + \mu}, \qquad \text{(Recovery rate, without } \alpha\text{)}$$

$$\Upsilon_{R_0}^{\delta} = -\frac{\delta}{\delta + \gamma + \mu}, \qquad \text{(Progression rate to cancer)}$$

$$\Upsilon_{R_0}^{\mu} = -\frac{\delta + \gamma + 2\mu}{\delta + \gamma + \mu}, \qquad \text{(Natural mortality rate)}$$

Parameter	Description	Values $(\text{year})^{-1}$
γ	Recovery rate due to natural immunity	0.2
δ	Progression rate of HPV to cervical cancer	0.008
μ	Natural rate of mortality	0.012

Table 3: Estimated parameter values and description of the model

Parameter	Sensitivity index
$\Upsilon_{R_0}^{\beta}$	1
$\Upsilon_{R_0}^{\Lambda}$	1
$\Upsilon_{R_0}^{\gamma}$	-0.90
$\Upsilon_{R_0}^{\delta}$	-0.036
$\Upsilon_{R_0}^{\mu}$	-1.05

Table 4: Sensitivity indices of $\mathcal{R}_0$ with respect to parameters given in Table 3

The sensitivity analysis of the basic reproduction number R_0 with respect to model parameters shows that the transmission rate β and recruitment rate Λ have the greatest influence, each with a sensitivity index of 1. This means that a 1% increase in either parameter leads to a 1% increase in R_0, since individuals who progress to the cancer class C are no longer contributing to new infections thus reducing the infectious population. Both the recovery rate γ and the natural mortality rate μ also have a negative impact on R_0, implying that faster recovery or higher death rates suppress disease transmission. In contrast, the immunity loss rate α has no effect on R_0, as its sensitivity index is zero.
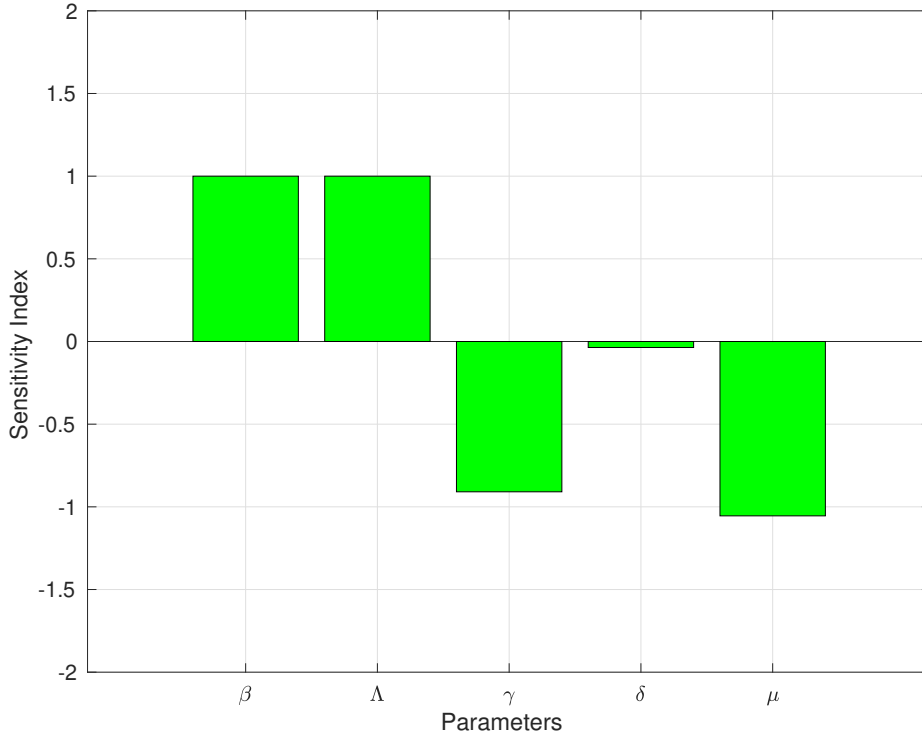
Figure 3: Sensitivity indices of R_0 with respect to model parameters

Partial Rank Correlation Coefficients (PRCC)

Parameter	Description	Values (year)$^{-1}$
Λ	Recruitment rate into the susceptible individuals	(5, 40)
β	Transmission rate of contact with individuals	(0.1, 1.0)
α'	Saturation factor	(0.005, 0.02)
γ	Recovery rate due to natural immunity	(0.01, 1.0)
δ	Progression rate of HPV to cervical cancer	(0.001, 0.6)
ξ	Death rate of individuals with cervical cancer	(0.1, 0.25)
μ	Natural rate of mortality	(0.01, 0.8)
α	Rate of loss of immunity	(0.01, 0.2)

Table 5: Estimated parameter values and description of the model (2.1)

The PRCC analysis the main factors driving disease transmission. The recruitment rate (Λ) and the transmission rate (β) emerge as the most influential parameters, suggesting that controlling new entries in the susceptible population and reducing contact-based transmission are the most effective ways to reduce R_0. In contrast, parameters such as the mortality rate (μ) and the progression rate (δ) have a minimal impact, emphasizing that while these factors are important for individual health outcomes, they do not significantly alter the dynamics of broader spread of the disease.
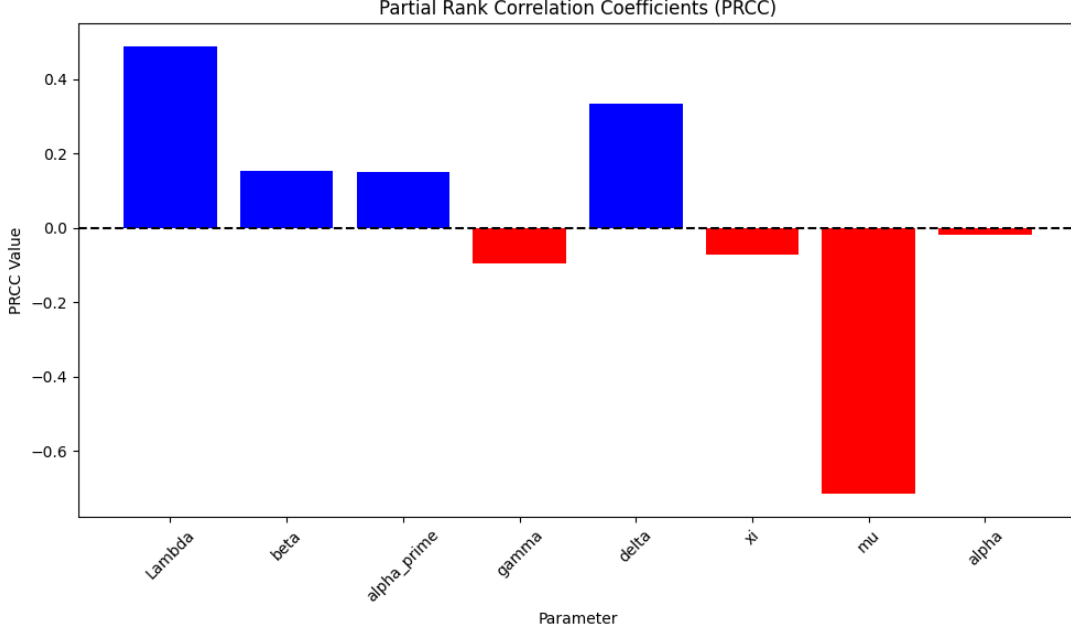
Figure 4: PRCC results capturing the sensitivity indices of parameters with R_0

9 Numerical simulations

In this section, we perform numerical simulations to meticulously examine the intricate dynamics of the deterministic model (2.1) to substantiate the theoretical insights expounded in the previous sections. Through careful selection of parameter values, we embark on a comprehensive exploration and analysis of the system's complete dynamical profile, encompassing aspects such as stability analysis. To execute numerical computations, we harness the computational capabilities offered by MATLAB, MATCONT and MATHEMATICA software tools.

Time Series for disease-free equilibrium

Here, we analyze the stability behavior of the Disease-Free Equilibrium (DFE) using the updated parameter values that satisfy the condition $\mu > 0.0765$, while maintaining similar system dynamics.

Parameter Values:

$$\Lambda = 36, \quad \beta = 0.30, \quad \mu = 0.08, \quad \alpha = 0.12, \quad \delta = 0.18, \quad \gamma = 0.4, \quad \xi = 0.2, \quad \alpha' = 0.01.$$

The basic reproduction number R_0 for this model is given by:

$$R_0 = \frac{\tilde{S} \cdot \beta}{\gamma + \mu + \delta}, \quad \text{where } \tilde{S} = \frac{S_0}{N_0}.$$

Substituting the values:

$$\tilde{S} = \frac{421.896}{451.815} \approx 0.9338, \quad \text{and } \gamma + \mu + \delta = 0.4 + 0.08 + 0.18 = 0.66,$$

$$\Rightarrow R_0 = \frac{0.9338 \cdot 0.30}{0.66} \approx 0.4246 < 1.$$

15

Thus, the basic reproduction number is below 1, suggesting that the infection will eventually die out.

The disease-free equilibrium is:

$$E_0 = (S^*, I^*, C^*, R^*) = (S^*, 0, 0, 0),$$

$$\text{where } S^* = \frac{\Lambda}{\mu} = \frac{36}{0.08} = 450.$$

Eigenvalues of the Jacobian at DFE:

$$\lambda_1 = -\mu = -0.08,$$

$$\lambda_2 = \frac{\beta \Lambda}{\mu N_0} - (\gamma + \mu + \delta = -0.3613,$$

$$\lambda_3 = -(\delta + \mu + \xi) = -(0.18 + 0.08 + 0.2) = -0.46,$$

$$\lambda_4 = -(\alpha + \mu) = -(0.12 + 0.08) = -0.20.$$

Since all eigenvalues are negative, the DFE E_0 is locally asymptotically stable under the modified parameter regime as well.
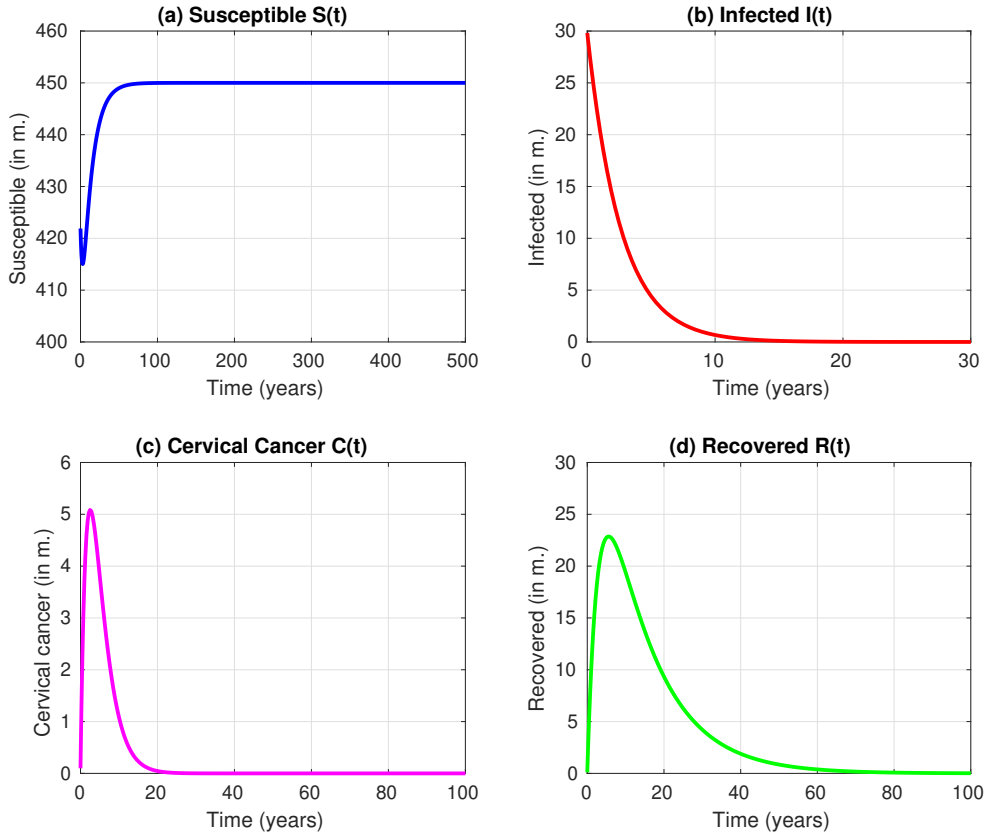

Figure 5: Stability analysis for Disease free Equilibrium $E_0(450, 0, 0, 0)$ with initial conditions $(421.896, 29.819, 0.0991, 0.1)$

Time series for endemic equilibrium

Now, the numerical simulation for the Endemic Equilibrium (EE) point corresponding to the following parameter values:

$$\Lambda = 8.8, \quad \beta = 0.41, \quad \mu = 0.012, \quad \alpha = 0.012, \quad \delta = 0.008, \quad \gamma = 0.2, \quad \xi = 0.001, \quad \alpha' = 0.5714$$

The basic reproduction number is calculated as:

$$R_0 = \frac{(S_0/N_0) \cdot \beta}{\gamma + \mu + \delta} \approx 1.7453 > 1.$$

Thus, the endemic equilibrium point is approximately:

$$E_1(S^*, I^*, C^*, R^*) \equiv E_1(403.79, 12.85, 18.24, 296.16).$$

The eigenvalues of the Jacobian matrix at E_1 are:

$$\lambda_1 = -0.0211 + 0.0141i,$$
$$\lambda_2 = -0.0211 - 0.0141i,$$
$$\lambda_3 = -0.0194,$$
$$\lambda_4 = -0.012.$$

Since all eigenvalues have negative real parts, the endemic equilibrium E_1 is locally asymptotically stable. Therefore, any small perturbations will decay over time and the system will return to equilibrium.
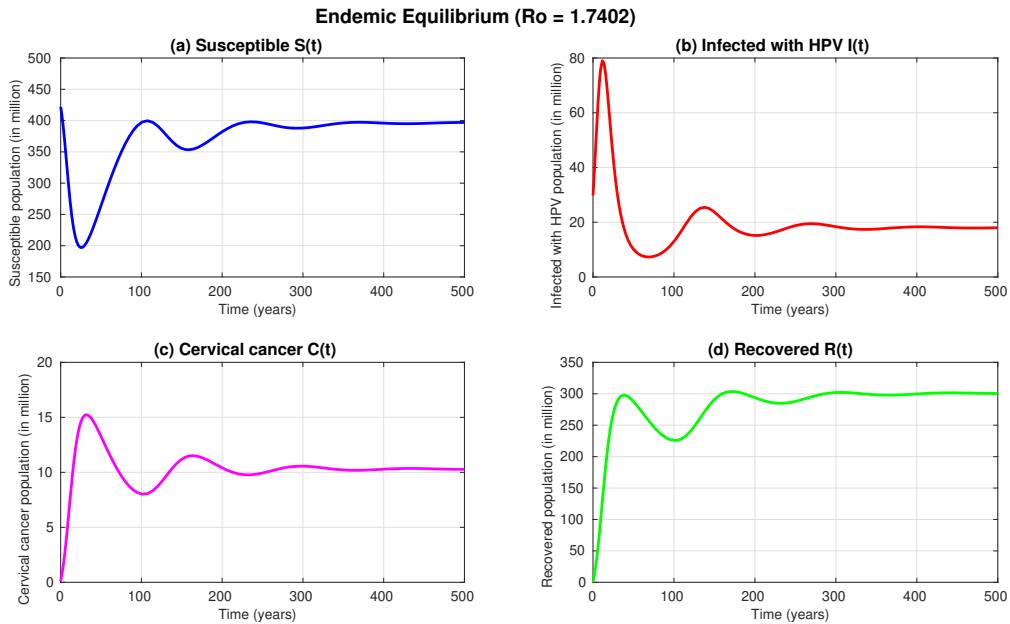

Figure 6: Stability analysis for Endemic Equilibrium $E_1(403.79, 12.85, 18.24, 296.16)$ with initial conditions $(421.896, 29.819, 0.0991, 0.1)$

article titlesec

17

7th Sem Work

Optimal Control Strategies

In this section, we extend our model to incorporate optimal control strategies that could help mitigate the spread of HPV infection and reduce cervical cancer cases. We introduce control measures and analyze their effectiveness through optimal control theory.

10.1 Model with Control Variables

We modify our original cervical cancer model by introducing two control variables representing public health interventions:

- $u_1(t)$: A prevention campaign (e.g., promoting HPV vaccination or safe practices) that reduces the HPV transmission rate, β. We model this as $\beta(1 - u_1(t))$.

- $u_2(t)$: An enhanced treatment program for HPV-infected individuals that increases the recovery rate, γ. We model this by adding a control-dependent recovery term, $u_2(t)I$.

The controlled system becomes:

$$
\begin{aligned}
\frac{dS}{dt} &= \Lambda - \frac{\beta(1 - u_1(t))SI}{1 + \alpha'I} - \mu S + \alpha R \\
\frac{dI}{dt} &= \frac{\beta(1 - u_1(t))SI}{1 + \alpha'I} - \gamma I - \delta I - \mu I - u_2(t)I \\
\frac{dC}{dt} &= \delta I - \xi C - \mu C \\
\frac{dR}{dt} &= \gamma I - \alpha R - \mu R + u_2(t)I
\end{aligned}
\tag{10.1}
$$

10.2 Objective Functional

Our goal is to minimize the number of infected individuals (I) and cancer cases (C), while also minimizing the cost of prevention (u_1) and treatment (u_2) programs. We define the total cost over a time period $[0, T_f]$ as:

$$
J[u_1, u_2] = \int_0^{T_f} \left(w_1 I(t) + w_2 C(t) + \frac{w_3}{2}u_1^2(t) + \frac{w_4}{2}u_2^2(t) \right) dt
\tag{10.2}
$$

where:

- $w_1 I + w_2 C$ represents the cost of the disease burden

- $\frac{w_3}{2}u_1^2 + \frac{w_4}{2}u_2^2$ represents the cost of implementing the controls, using a standard quadratic form

- w_i are positive weight constants to balance the terms

10.3 Hamiltonian Formulation

We formulate the Hamiltonian by combining the cost integrand with the controlled system using four adjoint variables: $\lambda_S, \lambda_I, \lambda_C,$ and λ_R.

$$
\begin{aligned}
H = {} & w_1 I + w_2 C + \frac{w_3}{2} u_1^2 + \frac{w_4}{2} u_2^2 \\
& + \lambda_S \left(\Lambda - \frac{\beta(1 - u_1)SI}{1 + \alpha' I} - \mu S + \alpha R \right) \\
& + \lambda_I \left(\frac{\beta(1 - u_1)SI}{1 + \alpha' I} - (\gamma + \delta + \mu + u_2)I \right) \\
& + \lambda_C \left(\delta I - (\xi + \mu)C \right) \\
& + \lambda_R \left((\gamma + u_2)I - (\alpha + \mu)R \right)
\end{aligned}
\tag{10.3}
$$

10.4 Adjoint System

We derive the differential equations for the adjoint variables by taking the negative partial derivative of the Hamiltonian with respect to each state variable.

$$
\begin{aligned}
\frac{d\lambda_S}{dt} &= -\frac{\partial H}{\partial S} = \lambda_S \left(\frac{\beta(1 - u_1)I}{1 + \alpha' I} + \mu \right) - \lambda_I \left(\frac{\beta(1 - u_1)I}{1 + \alpha' I} \right) \\
\frac{d\lambda_I}{dt} &= -\frac{\partial H}{\partial I} = -w_1 + (\lambda_S - \lambda_I) \left(\frac{\beta(1 - u_1)S\alpha'}{(1 + \alpha' I)^2} \right) + \lambda_I(\gamma + \delta + \mu + u_2) - \lambda_C \delta - \lambda_R(\gamma + u_2) \\
\frac{d\lambda_C}{dt} &= -\frac{\partial H}{\partial C} = -w_2 + \lambda_C(\xi + \mu) \\
\frac{d\lambda_R}{dt} &= -\frac{\partial H}{\partial R} = -\lambda_S \alpha + \lambda_R(\alpha + \mu)
\end{aligned}
\tag{10.4}
$$

with transversality conditions:

$$
\lambda_S(T_f) = 0, \quad \lambda_I(T_f) = 0, \quad \lambda_C(T_f) = 0, \quad \lambda_R(T_f) = 0
\tag{10.5}
$$

10.5 Optimal Controls

We characterize the optimal controls, u_1^* and u_2^*, by minimizing the Hamiltonian with respect to each control variable.

For u_1^*:

$$
\frac{\partial H}{\partial u_1} = w_3 u_1 + \lambda_S \left(\frac{\beta SI}{1 + \alpha' I} \right) - \lambda_I \left(\frac{\beta SI}{1 + \alpha' I} \right) = 0
\tag{10.6}
$$

Solving for u_1^*:

$$
u_1^* = \frac{1}{w_3}(\lambda_I - \lambda_S) \frac{\beta SI}{1 + \alpha' I}
\tag{10.7}
$$

For u_2^*:

$$
\frac{\partial H}{\partial u_2} = w_4 u_2 - \lambda_I I + \lambda_R I = 0
\tag{10.8}
$$

Solving for u_2^*:

$$u_2^* = \frac{I}{w_4}(\lambda_I - \lambda_R) \tag{10.9}$$

Since the controls must be bounded between 0 and 1, we apply the bounds:

$$u_1^*(t) = \max\left(0, \min\left(1, \frac{1}{w_3}(\lambda_I - \lambda_S)\frac{\beta SI}{1 + \alpha' I}\right)\right) \tag{10.10}$$

$$u_2^*(t) = \max\left(0, \min\left(1, \frac{I}{w_4}(\lambda_I - \lambda_R)\right)\right) \tag{10.11}$$

10.6   Numerical Solution and Interpretation

The optimal control problem can be solved numerically using iterative techniques:

1. Forward-backward sweep method:

   - Solve the state system forward in time with initial guesses for controls
   - Solve the adjoint system backward in time using the state values
   - Update the control values using the optimality conditions
   - Iterate until convergence

2. Expected outcomes:

   - u_1^* tends to be highest in early stages to prevent new infections
   - u_2^* may vary according to the prevalence of infection
   - The total infected and cancer populations should be reduced compared to the no-control scenario

This optimal control framework provides valuable insights for public health policy, indicating how resources should be allocated between prevention and treatment strategies over time to minimize both the disease burden and intervention costs.

10.7 Numerical Results: Effect of Optimal Controls

In all comparisons below, the **red solid line** denotes the *without control* (baseline) trajectory, and the **blue solid line** denotes the *with control* trajectory for the scenario under discussion.

By "without control" we mean the baseline model with no interventions applied:

$$u_1(t) = 0, \qquad u_2(t) = 0, \qquad t \in [0, T_f].$$

The different "with control" cases activate one or both controls within the admissible bounds $0 \leq u_i(t) \leq 1$ and follow the optimality system described earlier.

10.7.1 With Vaccination Control vs. Without Vaccination

Mechanism of vaccination control.

- **Vaccination (u_1):** Directly moves susceptibles to the recovered class, providing immunity without infection. No awareness effect is present ($u_2 = 0$).

With vs. Without Control: What changes happen.

- **Susceptible (S):** With vaccination, S drops rapidly as individuals are immunized and stabilizes at a low level; without vaccination, S decreases mainly through infection and remains lower.

- **Infected (I):** With vaccination, I collapses quickly and remains near zero, as the susceptible pool is depleted by immunization; without vaccination, I peaks higher and declines slowly.

- **Cancer (C):** With vaccination, C is almost eliminated, since infections are rare; without vaccination, C peaks higher and decays slowly.

- **Recovered (R):** With vaccination, R rises sharply and stabilizes at a high value, reflecting widespread immunity; without vaccination, R grows more slowly, only as a result of recovery after infection.

About the graph. The figure compares S, I, C, and R with (**blue**) and without (**red**) vaccination. Vaccination causes rapid decline of infection and cancer, and a swift rise in recovered, consistent with $u_1^*(t) > 0$ and $u_2(t) = 0$.
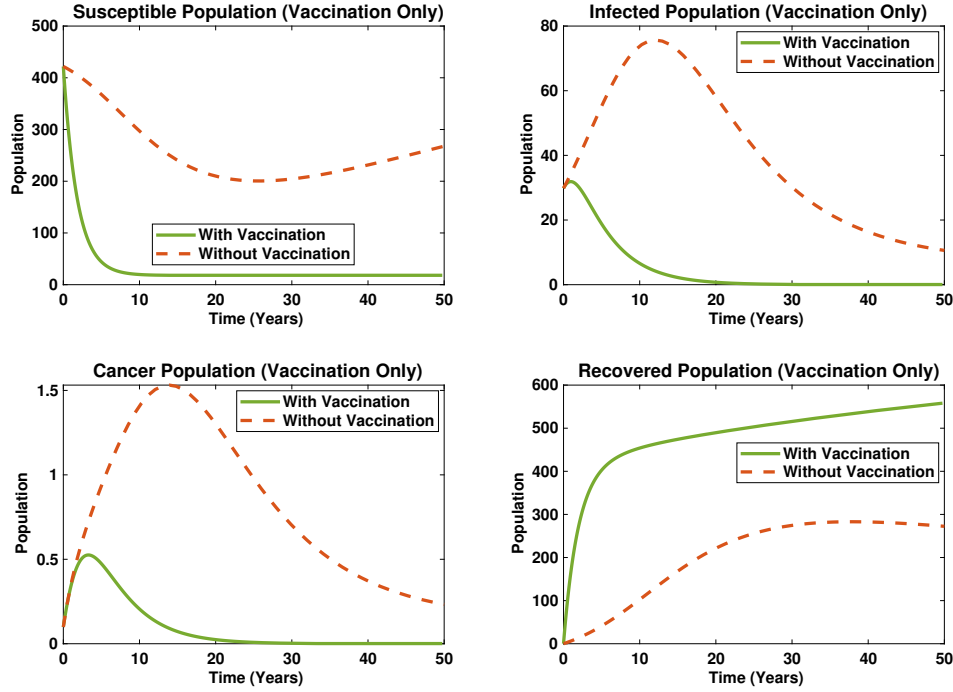
Figure 7: Vaccination vs. no vaccination. Blue: with vaccination ($u_1^* > 0$, $u_2 = 0$). Red: without vaccination (baseline). Vaccination directly immunizes, reduces infections and cancer, and builds lasting population immunity.

10.7.2 With Awareness Control vs. Without Awareness Control

Mechanism of awareness control.

- **Awareness (u_2):** Reduces transmission rate by promoting preventive behaviors and knowledge, so fewer susceptibles become infected. No vaccination effect is present ($u_1 = 0$).

With vs. Without Control: What changes happen.

- **Susceptible (S):** With awareness, S declines more slowly and stabilizes higher, as fewer people get infected due to behavioral change; without awareness, S drops faster.

- **Infected (I):** With awareness, I peaks lower and declines faster, since transmission is reduced; without awareness, I peaks higher and persists longer.

- **Cancer (C):** With awareness, C is much lower, reflecting fewer prolonged infections; without awareness, C peaks higher.

- **Recovered (R):** With awareness, R rises slowly and plateaus at a lower value, since fewer people get infected and need to recover; without awareness, R increases more due to higher infection rates.

About the graph. The figure shows S, I, C, and R for **blue (with awareness)** and **red (without awareness)**. Awareness keeps the susceptible pool higher, suppresses infections and cancer, and results in a lower recovered population—consistent with $u_2^*(t) > 0$ and $u_1(t) = 0$ acting by reducing transmission.
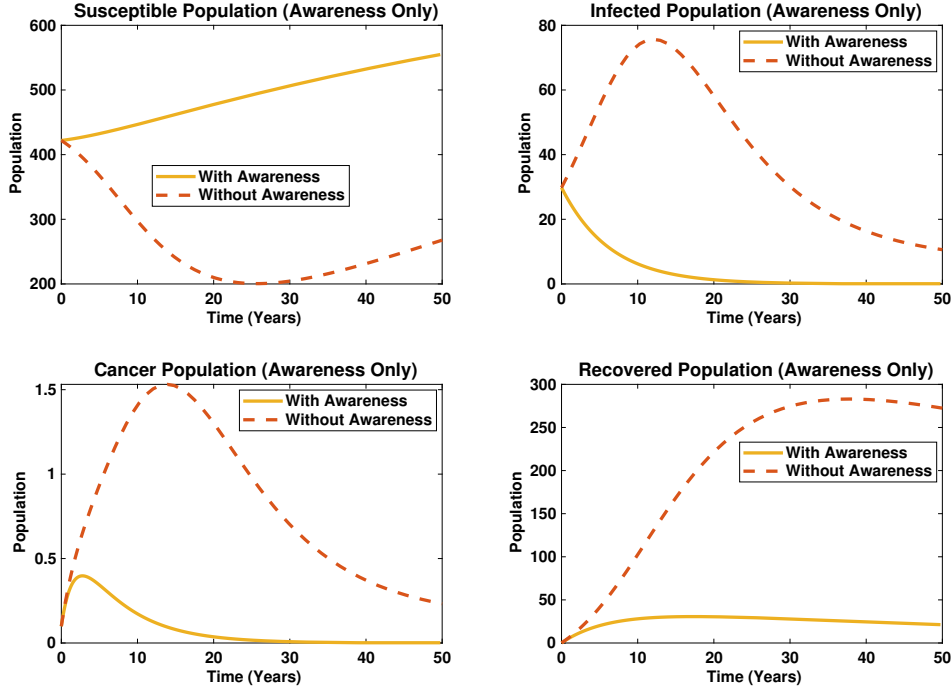

Figure 8: Awareness vs. no awareness. Blue: with awareness ($u_1 = 0$, $u_2^* > 0$). Red: without awareness (baseline). Awareness reduces transmission, keeps more people healthy, and suppresses infection and cancer.

10.7.3 With General Control vs. Without General Control

Mechanism of controls.

- **Vaccination (u_1):** Directly moves individuals from susceptible to recovered, granting immunity without infection.

- **Awareness (u_2):** Reduces the transmission rate by changing behavior and increasing knowledge, so fewer susceptible individuals become infected.

With vs. Without Control: What changes happen.

- **Susceptible (S):** With general control, S decreases more slowly and stabilizes higher, as vaccination immunizes susceptibles and awareness prevents new infections; without control, S falls rapidly due to high infection rates.

- **Infected (I):** With control, I peaks lower and earlier, then declines rapidly because fewer are at risk and transmission is suppressed; without control, I peaks higher and later.

24

- **Cancer (C):** With control, C remains low, since there are fewer and shorter infections to progress to cancer; without control, C peaks higher and decays more slowly.

- **Recovered (R):** With control, R increases rapidly and stabilizes at a high level due to vaccination and reduced infections; without control, R grows mainly through recovery after infection and stabilizes later.

About the graph. The figure plots S, I, C, and R over time for both cases. **Blue (with control)** shows a lower, earlier infection peak, suppressed cancer, higher susceptibles, and rapid stabilization of recovered. **Red (without control)** shows higher infection and cancer burdens and slower stabilization.
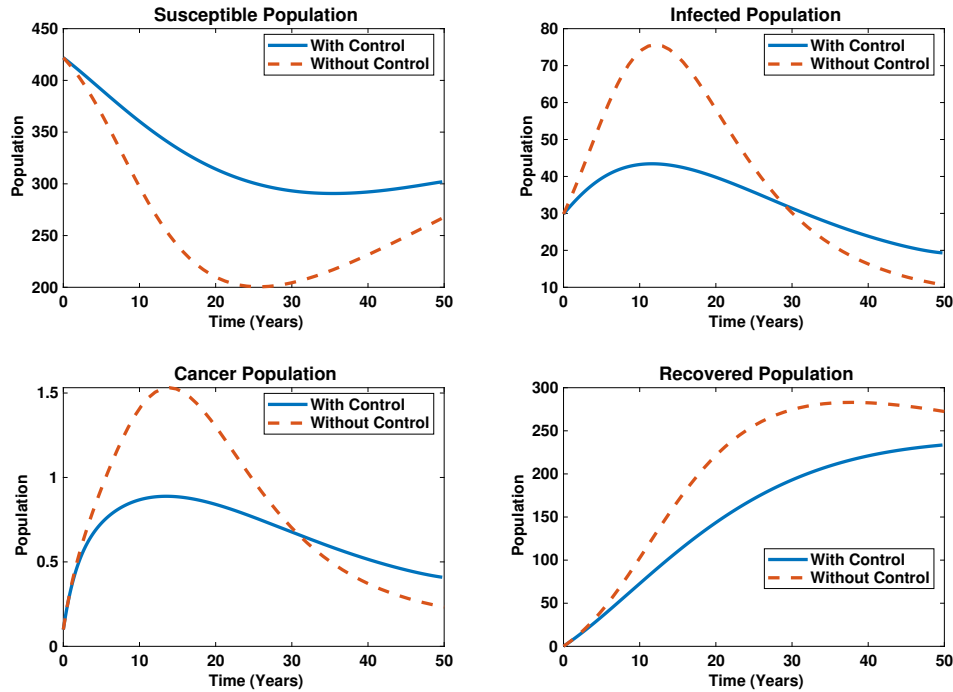

Figure 9: General control vs. no control. Blue: with general control (vaccination + awareness). Red: without control (baseline).

Summary. Across all three scenarios, the control case (blue) outperforms the baseline (red). Vaccination yields the fastest and most durable reduction in infections and cancer; general control combines prevention and treatment to flatten and shorten the epidemic while suppressing cancer; awareness (modeled here via enhanced recovery) also reduces burden and complements the other measures. In practice, combining these controls provides the strongest and most sustainable impact.

Conclusion

- This project developed a mathematical model to study the spread of HPV infection and its progression to cervical cancer using a system of differential equations.

- The basic reproduction number R_0 was derived to determine the conditions for disease persistence or elimination.

- Stability analysis showed that:

  - When $R_0 < 1$, the disease-free equilibrium (DFE) is globally stable, meaning the infection dies out.
  - When $R_0 > 1$, an endemic equilibrium (EE) appears, indicating the infection persists in the population.

- A bifurcation analysis at $R_0 = 1$ confirmed a transcritical bifurcation, where the stability of equilibria shifts as R_0 crosses the threshold.

- Numerical simulations illustrated the time evolution of different population groups (susceptible, infected, cancer cases, and recovered individuals), validating the theoretical findings.

- The study emphasizes that reducing HPV transmission (e.g., through vaccination and treatment) can lower R_0 and prevent cervical cancer cases.

- Future improvements could include:

  - Incorporating vaccination strategies and age-structured models.
  - Analyzing seasonal effects and external interventions.
  - Extending the model to study co-infections with other diseases.

- Overall, this project highlights how mathematical modeling helps understand disease dynamics and supports public health strategies to control HPV and cervical cancer.

References

[1] World Health Organization. Global strategy to accelerate the elimination of cervical cancer as a public health problem (2020). Available at: `https://www.who.int/publications/i/item/9789240014107`. Accessed: 05 March 2021.

[2] Ferlay, J., Ervik, M., Lam, F., Colombet, M., Mery, L., Piñeros, M., Znaor, A., Soerjomataram, I., Bray, F. (2020). Global Cancer Observatory: Cancer Today. Lyon, France: International Agency for Research on Cancer. Available at: `https://gco.iarc.fr/today`. Accessed: 05 March 2021.

[3] Bruni, L., Albero, G., Serrano, B., et al. ICO/IARC Information Centre on HPV and Cancer (HPV Information Centre). Human Papillomavirus and Related Diseases in India. Summary Report 10 December 2018. `https://hpvcentre.net/`. Accessed: 05 March 2021.

[4] Kermack, W.O., McKendrick, A.G. (1927). Contributions to the mathematical theory of epidemics. *Proc. R. Soc. Lond. Ser. A*, 115, 700–721. `https://doi.org/10.1098/rspa.1927.0118`.

[5] Sarkar, K., Khajanchi, S., Nieto, J.J. (2020). Modeling and forecasting the COVID-19 pandemic in India. *Chaos Solitons Fractals*, 139, 110049–16. `https://doi.org/10.1016/j.chaos.2020.110049`.

[6] Lee, S.L., Tameru, A.M. (2012). A mathematical model of Human Papillomavirus (HPV) in the United States and its impact on cervical cancer. *J. Cancer*, 3, 262–268. `https://doi.org/10.7150/jca.4161`.

[7] Franceschi, S., Rajkumar, R., Snijders, P., et al. (2005). Papillomavirus infection in rural women in southern India. *Br. J. Cancer*, 92(3), 601–606. `https://doi.org/10.1038/sj.bjc.6602348`.

[8] Indian Council of Medical Research (2021). Consensus document for management of cancer cervix. Available at: `https://main.icmr.nic.in/sites/default/files/reports/Cervix`.

[9] Huo, H.F., Chen, R., Wang, X.Y. (2016). Modelling and stability of HIV/AIDS epidemic model with treatment. *Appl. Math. Model.*, 40(13–14), 6550–6559. `https://doi.org/10.1016/j.apm.2016.01.054`.

[10] Su, R., Yang, W. (2021). Global stability of a diffusive HCV infections epidemic model with nonlinear incidence. *J. Appl. Math. Comput.* `https://doi.org/10.1007/s12190-021-01637-3`.

[11] Tyagi, S., Martha, S.C., Abbas, S., Debbouche, A. (2021). Mathematical modeling and analysis for controlling the spread of infectious diseases. *Chaos Solitons Fractals*, 144, 110707. `https://doi.org/10.1016/j.chaos.2021.110707`.

[12] Ross, R. (1911). The Prevention of Malaria, 2nd edn. John Murray, London.